Σ

SPE 30790

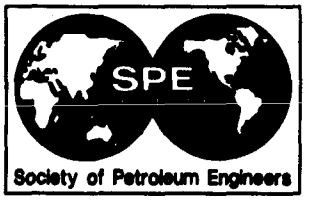

An Integrated 3D Model for Underground Coal Gasification

E.N.J. Biezen, SPE, Delft U. of Technology, Centre for Technical Geoscience (CTG), and J. Bruining, SPE, Delft U. of Technology, CTG, and J. Molenaar, Delft U. of Technology

This paper was prepared for presentation at the SPE Annual Technical Conference & Exhibition held in Dallas, U.S.A., 22-25 October, 1995.

Abstract

Underground coal gasification has received renewed interest in both Western and Eastern Europe because of the vast amounts of otherwise unminable coal deposits that occur on the European continent. A field test is currently being held in Spain, and other countries have also shown interest in this method of utilizing coal resources.

In this study we have developed a model to combine reactive heat and mass transport together with thermo-mechanical failure behavior. In the model, we use multigrid methods to solve the flow equations in the entire domain. This is combined with thermo-mechanical failure properties of both coal and rock overlying the coal formation. With this approach, a 3D picture of the development of an underground coal gasifier is obtained, and the influence of well-layout and the sensitivity of the process to other model parameters can be investigated in detail, with high computational efficiency.

The model consists of two modules: The first module solves the flow equations in the entire flow domain. The second module selects a block of coal for gasification and a block of coal and/or rock for thermo-mechanically induced spalling. Other features such as ash content, the possibility of including heterogeneities, and natural convection-driven cavity gasification are also incorporated in the model.

Introduction

Underground coal gasification (UCG) is a method of utilizing the vast otherwise unminable coal resources. Deep lying, thin coal seams such as occur in North-Western Europe can possibly be economically recovered by the application of UCG in combination with standard directional and horizontal drilling techniques. A typical configuration consists of a horizontal injection well with a vertical producer. Prior to the gasification step a linkage path is created between injector and producer using, for example, reverse combustion to char the coal,[1] or hydraulic fracturing. The gasification step starts with ignition of the coal and the injection of air or air enriched with oxygen. Both permeable bed gasification and natural convection driven surface gasification will occur. When the gas quality deteriorates the injection well is burnt to allow injection further upstream.[2] This technique is called CRIP, i.e., Controlled Retraction Injection Point. The situation during the first CRIP step is schematically shown in Fig. 1. The successful UCG field tests were designed for two or more of these CRIP steps.[3,4]

The design of a field test and its interpretation would greatly benefit from a simple dedicated simulator. The model must be able to describe the development from the early stages of gasification to a fully developed gasifier. The field test in Pricetown, U.S.A. shows a possible mature configuration of a gasifier; gases percolate through ash and rock debris to a teardrop shaped channel where natural convection driven surface gasification takes place. A model for the initial stages has been developed by Britten and Thorsness.[3,5] Their model was successful in describing field tests in thick coal layers.[4] For economic gasification of thin coal layers, however, the cavity must develop to cover a radius much larger than the layer thickness. This means that natural convection driven cavity surface gasification becomes increasingly important with respect to the permeable bed gasification that dominates the initial stages. Deviations from the cylindrical shape of the gasifier are important for the attainable areal sweep efficiency. The model of Britten and Thorsness was never meant to include these two aspects.

The cavity or channel approach forms the basis for several simulation models that describe the growth of a gasification cavity in coal seams.[6-9] Due to the complexity of the gasification process, all these models rely on the assumption that a cavity exists. Most of these models only describe the expansion of the cavity due to chemical reactions, and disregard mechanical failure

mechanisms. Van Batenburgs' model[10,11] includes both chemical reactions and rock failure, but its purpose was to show that acceptable gas compositions could be attained in cavity gasification. It does not predict a limit for areal sweep efficiency.

In this paper we present a 3D model that can: (1) describe the transition from the early stages to a fully developed gasifier, and (2) predict the areal sweep efficiency. It is a 3D extension of a previously described 2D model.[12] Main differences (apart from the extra dimension) with the earlier presented 2D model lie in the fact that a pressure formulation is used in stead of the stream function approach. In the model the essential features of the underground gasification process are captured. Many aspects have already been mentioned in the 2D version,[12] but are repeated here to avoid tedious cross-referencing. We will address the influence of ash permeability on overall cavity development, as well as the thermo-mechanically induced spalling of both roof rock and coal.

The model includes aspects of permeable bed gasification, natural convection driven cavity surface gasification and roof-failure mechanisms. Important parameters are the ash content, permeabilities (of ash, roof debris, and char), well outlay and injection strategy. The model calculates the form and shape of the cavity. The long term development of the cavity is dominated by natural convection driven cavity gasification.

The main applications of this 3D model are the design and evaluation of underground coal gasification field trials, as well as the extrapolation of field test results to the deep-lying thin coal seams such as occur in North-Western Europe.

Physical Model

Structural configuration. Consider a horizontal coal layer with thickness h, length L, and width W with a rock layer on top of it. A 3D representation is shown in Fig. 2, and a vertical cross section at $W/2$ is shown in Fig. 1. There are four subregions: the ash region Ω_A, the coal region Ω_C, the void region Ω_V, and the cap-rock region Ω_R.

The gasified region Ω_A, where all coal has been consumed, consists of ash and spalled rock. No distinction between ash and spalled rock is made. The gasified region has the injection temperature. The downstream coal region Ω_C contains unreacted coal and char. We disregard heat losses and assume that Ω_C has a constant (product gas-) temperature.

There are four interfaces. Γ_{vr} is the interface between the rock and the void. Γ_{vc} and Γ_{ac} are the interfaces between void and coal, and between ash and coal, respectively. $\Gamma_{vc} \cup \Gamma_{ac}$ comprise the interface between the gasified regions $\Omega_A \cup \Omega_V$ and the coal region Ω_C. Finally, Γ_{va} is the interface between void region Ω_V and ash region Ω_A. We use the term cavity to denote the total void space. The whole domain consisting of ash, char, coal, rock, and void, is indicated by Ω.

Injection occurs at the bottom of the coal seam from the tip of a horizontal injection well. Production occurs via a vertical producer which is completed over the entire height of the coal layer.

Flow modeling. The underground reactor represented by the domain Ω is modeled as a heterogeneous permeability field. The flow is governed by Darcy's equation. We disregard gravity effects due to small gas densities. Since only permeability ratios are important here, we measure all permeabilities by a reference quantity k_{ref}. The essentially impermeable behavior of unaffected coal and rock is modeled with a low permeability. The char, ash, and spalled rock permeabilities are model parameters. Finally, the void is assigned a high permeability, to model a constant pressure condition.

The injection and production boundary conditions are a constant injection rate and a constant production pressure, respectively. In the model we distinguish two temperature regions: an upstream region with the injection temperature and a downstream region with the product gas temperature. The temperature dependence of the gas viscosities is given by:[13] $\mu_u/\mu_d = (T_u/T_d)^{0.634}$. We disregard the composition dependence of the gas viscosity μ. More sophisticated approximations are not warranted in view of the uncertainty of the permeability distribution.

The flow equations are solved with a probabilistic method. Probabilistic methods were introduced for problems of reservoir engineering interest by Patterson[14] who showed the analogy between diffusion-limited aggregation (DLA) of colloids and flow in porous media. Both processes are described by Laplace's equation, with similar boundary conditions. DeGregoria[15] and King and Scher[16] extended the DLA approach to more sophisticated flow problems in porous media.

King[17] has shown that the probabilistic method gives similar results as deterministic methods for a variety of stable displacement processes. King's work is based on a stream function approach. Frick et al.[18] use a pressure formulation. Probabilistic methods are highly suitable for unstable situations. For stable situations a deterministic solution method should lead to essentially the same results.

Permeable bed gasification reactions and gas properties. Prior to gasification a link i.e. a permeable path is made between the injection well and the production well. After linkage, a cavity starts to grow at the point where air or air enriched with oxygen is injected. Part of the gasification takes place in the permeable coal, and another part at the coal surface. The injected gas reacts either directly or indirectly with permeable coal. By direct reaction we mean that the injected gas only reacts with coal and does not enter the cavity. Part of the gas, however, reacts indirectly with the coal. Indeed some gas with the injection composition and temperature enters the cavity before it can react with coal. It then reacts with the omnipresent combustible gases to form hot combustion products, e.g. CO_2 and H_2O.

Part of the combustion products and remaining oxygen (if there is insufficient combustible gas) react at the coal wall driven by natural convection flows (cavity gasification; see below). The other part reacts with the coal between the cavity wall through which it is flowing and the production well (indirect permeable bed gasification). In spite of this, no distinction is made between direct and indirect permeable bed gasification. We merely use a parameter (P) to define how many carbon atoms react with one molecule of oxygen (O_2).

Because of the reactions the mass flux increases by addition of coal atoms to the gas. If gas reacts indirectly we can (owing to the high cavity permeability) equivalently concentrate all mass flux increase at the interface Γ_{vc} without affecting the flow field. We assume a constant product gas composition. Thus the ratio of the mass flux downstream and the mass flux upstream of the interfaces $\Gamma_{vc} \cup \Gamma_{ac}$ is constant. Furthermore we assume ideal gas behavior. The temperature of the product gas is the adiabatic flame temperature.

Cavity gasification by surface reactions. Cavity gasification is a complex process.[10,11,19] A detailed treatment is outside the scope of this article. The coal surface bounding the cavity reacts with the gases in the cavity. For sufficiently high temperatures the coal consumption rate is determined by the mass transfer rate through the boundary layer between the coal and the cavity. The forced convection flow in the cavity is negligible with respect to the natural convection flow.

For turbulent natural convection flows, i.e., at high Rayleigh numbers ($\mathrm{Ra} \geq 1 \cdot 10^{10}$), the transfer rate is constant: $k_f = 280\ \mathcal{D}\,[\mathrm{m^3/m^2 s}]$, where $\mathcal{D}[\mathrm{m^2/s}]$ denotes the molecular diffusion coefficient. The value of k_f is distributed relatively uniformly over the cavity.[19] The reaction rate $r = k_f\, P\, [O_2]\, M_c\, [\mathrm{kg\,carbon/m^2 s}]$, where $[O_2]$ is the molar oxygen concentration. The composition in the cavity may differ from the injection composition, but this will be disregarded as oxygen is replaced by carbondioxide which also reacts at the coal wall.

Coal and roof failure. Three mechanisms of roof failure are distinguished, viz. rock/coal spalling, melting and large scale roof collapse due to stress concentrations near the side boundaries of the cavity. Large scale roof collapse occurs when a considerable part of the roof span is unsupported. The critical span depends on the rock mass properties of the roof. The effect is less important at the initial stages of the gasification process and has not been taken into account.

Spalling is the chipping of rock induced by thermal and mechanical stresses.[20] Spalling occurs both for coal and rock. High spall rates develop only in rock/coal exposed to cavity temperatures exceeding 500°C. Due to the high temperature and pressure inside the cavity spalled coal blocks are immediately gasified.[5] We assume that spalling occurs at a constant rate. In our present calculations we use a spatially uniform spall rate. Spalling is introduced in the model as a local phenomenon. The spall locations are determined with a probabilistic method. The spall rates for rock and coal are model parameters. Melting effects can be modeled with enhanced spall rates and a low chipped rock permeability.

Cavity evolution. The procedure to determine the cavity evolution is as follows: Let the distribution of ash, void, and coal be given at a certain time. This geometry defines the permeability distribution. For the given permeability distribution we determine the flow field by applying Darcy's equation. As the coal consumption rate is small with respect to the gas velocities we can assume (quasi) stationary flow conditions. Coal is consumed at the interfaces $\Gamma_{vc} \cup \Gamma_{ac}$ at a rate proportional to the normal flux on the interface. At the cavity boundary an extra amount of coal is gasified due to natural convection driven surface gasification. Finally, all spalled coal is immediately gasified.

The volume of gasified coal becomes void space to be added to the cavity, and its ash is displaced vertically to the bottom of the cavity. The ash-void interface Γ_{va} is displaced downward when the coal beneath it is gasified. The rock and coal exposed to the cavity spall at a constant rate and also fall vertically downward. The volume of spalled rock/coal per unit original rock/coal volume are model parameters. The permeability distribution is updated and the calculation procedure enters the next time step.

Model equations

Generalized mass flux vector. A generalized mass flux vector $\vec{j}$ is defined by

$$\vec{j} = m\rho\vec{q} \quad \begin{cases} m = \frac{1}{\chi} & \text{in } \Omega_C \\ m = 1 & \text{in } \Omega_A \cup \Omega_R \cup \Omega_V \end{cases} \quad \ldots\ldots (1)$$

where $\vec{q}$ is the specific discharge and ρ is the density of the gas. The ratio χ between the mass flux downstream and the mass flux upstream of the interface between $\Omega_A \cup \Omega_V$ and Ω_C is constant. A similar ratio also occurs in steam drive.[21] The (stationary) conservation law reads $\mathrm{div}\ \vec{j} = 0$ in the whole domain Ω or

$$\begin{aligned} &\mathrm{div}\ \vec{j} = 0 && \text{in } \Omega \\ &j_{A,n} = j_{C,n} && \text{on } \Gamma_{ac} \\ &j_{V,n} = j_{C,n} && \text{on } \Gamma_{vc} \end{aligned} \quad \ldots\ldots (2)$$

where $j_{A,n}$ and $j_{V,n}$ are the normal components of the upstream generalized mass flux vector at Γ_{vc} and Γ_{ac}, respectively, and $j_{C,n}$ is the downstream generalized mass flux. Note that $(\rho q)_{A,n} \neq (\rho q)_{C,n}$ and $(\rho q)_{V,n} \neq (\rho q)_{C,n}$.

Darcy equation and pressure equation. Substitution of Darcy's equation in Eq. 1 gives

$$\vec{j} = -\rho \frac{k\,m}{\mu} \mathrm{grad}\, p \quad \text{in } \Omega. \quad \ldots\ldots (3)$$

The viscosity has two different values, viz. μ_u in the upstream region ($\Omega_A \cup \Omega_R \cup \Omega_V$) and μ_d in the downstream region (Ω_C). Substitution of Eq. 3 into Eq. 2 leads to the pressure equation

$$\begin{aligned} &\text{div}\ \frac{\rho k}{\mu_d \chi}\text{grad}\, p = 0 \quad \text{in } \Omega_C \\ &\text{div}\ \frac{\rho k}{\mu_u}\text{grad}\, p = 0 \quad \text{in } \Omega_A \cup \Omega_R \cup \Omega_V \end{aligned} \qquad \ldots\ldots\ldots (4)$$

Owing to the introduction of the generalized mass-flux vector we can derive one single pressure equation for the whole domain. The boundary conditions are the prescribed injection rate at the injection well, the constant production pressure and no-flow boundary conditions at the outer boundary of the domain Ω. Once the pressure field is known we determine by the application of Darcy's Eq. 3 the flow field $\vec{j}$ at the interfaces $\Gamma_{vc} \cup \Gamma_{ac}$.

Cavity development. We assume that the interfaces can be parametrized as a function of the x- and y-coordinates, i.e., $\gamma_{\alpha\beta} = \gamma_{\alpha\beta}(x, y, t)$ where $\gamma_{\alpha\beta}$ denotes the z-coordinate of the interface between Ω_α and Ω_β, with α, β = ash, coal, void, rock. The interface heights $\gamma_{\alpha\beta}(x, y, t)$ are only defined for those values of x and y that are physically relevant. The equations of motion of the interfaces read

$$\begin{aligned} \frac{\partial \gamma_{vr}}{\partial t} &= \frac{\lambda_{rock}}{a_{vr}} && \text{on } \Gamma_{vr} \\ \frac{\partial \gamma_{vc}}{\partial t} &= \frac{\omega(\rho q)_{V,n} + P k_f \frac{M_c}{\rho_{coal}} \frac{fp}{RT} + \lambda_{coal}}{a_{vc}} && \text{on } \Gamma_{vc} \\ \frac{\partial \gamma_{ac}}{\partial t} &= -\frac{1}{a_{ac}} \omega(\rho q)_{A,n} && \text{on } \Gamma_{ac} \\ \frac{\partial \gamma_{va}}{\partial t} &= \varsigma \frac{\partial \gamma_{vr}}{\partial t} + \nu \frac{\partial \gamma_{vc}}{\partial t} + (1-\nu) \frac{\partial \gamma_{ac}}{\partial t} && \text{on } \Gamma_{va} \end{aligned} \qquad (5)$$

In Eq. 5 the terms λ_{rock} and λ_{coal} represent the spalling of rock and coal, respectively. The factor $a_{\alpha\beta}$ denotes the projected area on a horizontal plane from a unit exposed surface. The terms $\omega(\rho q)_{A,n}$ and $\omega(\rho q)_{V,n}$ denote the coal that is gasified due to permeable bed gasification reactions and $(\rho q)_{V,n}$ is the mass flux perpendicular to Γ_{vc}, i.e., cavity/coal interface. $(\rho q)_{A,n}$ is the mass flux perpendicular to Γ_{ac}, i.e., the ash/coal interface. ω is the volume of coal gasified per unit mass of gases.

The term $P k_f \frac{M_c}{\rho_{coal}} \frac{fp}{RT}$ represents the coal that is gasified owing to the natural convection of gases in the cavity, f denotes the fraction of oxygen in the injection gas, ρ_{coal}/M_c is the molar density of coal, and $\frac{fp}{RT}$ is the molar concentration of oxygen in the injection gas.

$\frac{\partial \gamma_{va}}{\partial t}$ consists of positive terms due to the spalling of rock and ash originating from the spalled/gasified coal, and a negative term due to gasification underneath it. ν is the volume of ash per unit volume of coal gasified. ς represents the volume of spalled rock at the cavity floor that originated from a unit volume of roof-rock.

Numerical model

The numerical model calculates the pressure field at successive time steps. The bottom half of the reactor consists of coal and the top half of roof rock. At each time step we calculate the pressure field (see the Appendix), and from it the generalized mass flux field. We have used the pressure formulation for the extension of the model to 3D. With the calculated flow field the cavity development for a single time step is calculated.

To this end we could use the mass fluxes normal to the void/coal interface Γ_{vc} and the ash/coal interface Γ_{ac} directly in the equation of motion, Eq. 5, but a deterministic approach does not recognize the possible unstable character of the process. The advantage of the probabilistic method is that it constantly perturbs the solution. Therefore the probabilistic method readily detects unstable situations by giving different answers for different realizations.[22] In deterministic simulators noise has to be introduced to detect unstable behavior.[23]

The procedure (for details see the Appendix) to determine the cavity development for a single time step is as follows: first we calculate the total flow, Q, through all coal/char faces which are exposed to either void or ash, see also Fig. 3. Then we use a random number generator[24] to draw a single random number, $\mathcal{R}_1$, uniformly distributed between zero and one. Subsequently, we repeat the summation through the exposed coal/char faces until the value $\mathcal{R}_1 Q$ is reached. At this location the block of char or coal is gasified and a corresponding amount of ash is released. The ash falls down and accumulates at the bottom of the cavity.

At specific intervals, depending on the coal spall rate, a second and third random number are drawn. These random numbers specify the (x,y) location (column) of a coal block, which can spall if there is cavity directly below it. The spalled coal block is gasified immediately[5] and its ash content is released and accumulates at the bottom of the cavity.

In the same way two other random numbers select a block of rock for spalling. It should again be noted that only blocks of rock with surfaces exposed to the cavity can spall. Indeed, in the early stages of cavity growth no rock can spall. The spalled rock is released and accumulates as "ash" at the bottom of the cavity. An expansion factor can be assigned to the spalled material, to account for its increase in porosity.

Finally, a small portion of the coal surface exposed to the cavity is removed to account for the natural convection driven surface gasification. The ensuing ash accumulates below. The void/ash interface is accommodated so that no void is beneath it. With the updated cavity a new pressure field is calculated and the new velocities are determined. Subsequently, the cavity development is determined for the next time step, etc.

Iterative solution of pressure equation. The pressure equation is a 3D elliptic equation that has to be solved every time step. In the model we use the multigrid method that was developed by Molenaar.[25,26] This

method is especially designed for problems with strong anisotropies and heterogeneities. It is based on block Gauss-Seidel relaxation and a special averaging method for the definition of the coarse grid problems. The multigrid method is an efficient and robust solver for the pressure equation.

Example calculations

To illustrate the model we present some example 3D calculations for a UCG reactor represented by a 16×16×16 grid. The grid consists of eight bottom coal layers. On top of the eight coal layers are eight layers of roof rock with a low permeability. A schematic of the initial simulation domain is shown in Fig. 2. An aspect ratio $h/L = h/W = 1/2$ was used. A coal layer thickness of 4 meter is considered.

The example calculations investigate the influence of ash permeability, and coal and rock spall rates on the growth of an underground gasification cavity. For all cases but one (Case G) it is assumed that the whole coal zone has been charred prior to the gasification, leading to a permeability that equals k_{ref} in the entire coal zone. Other realizations (with different seeds for the random number generator) show qualitatively the same behavior as the results presented below. The configuration used is representative for the initial stages of gasification in the first CRIP manoeuvre.

Furthermore, we used a char permeability of k_{ref}, a roof rock permeability of $10^{-3}k_{ref}$, and a void permeability of $10^{5}k_{ref}$. A listing of the input parameters common to all simulations is shown in Table 1. For each time step, $\mathcal{N}$ pairs of random numbers $\mathcal{R}_2$ and $\mathcal{R}_3$ are drawn to obtain possible coal spalling sites. This leads to a coal spall rate probability for one column (out of the 256 columns $h\,\Delta x\,\Delta y$) of $\frac{\mathcal{N}}{256}$ per gasified coal block. A high spall rate corresponds to a high value of $\mathcal{N}$. Spalling from the roof can occur if this column intersects with the cavity. The average spall rate for rock was taken equal to the average coal spall rate for all cases considered here.

Figures 4 through 10 show calculation results on a 16×16×16 grid. In the figures, only the bottom (coal) half is shown in a 3D view. The ash region that forms at the bottom of the cavity during the simulations, is omitted as well, for reasons of clarity. The injection/production well layout is shown schematically in Fig. 2. In Table 2 a listing is given of the remaining input parameters which were used for each of the Cases A through G.

Figures 4 and 5, Case A and B, show a 3D view of the gasified region, without spalling and with considerable spalling, respectively. Both cases have the same (high) ash permeability and ash content. Fig. 4 (Case A) shows an evenly developed cavity which has grown steadily upwards to the low permeable roof rock (not shown in the picture). In contrast, Fig. 5 shows a cavity which has grown mostly to one side of the simulation domain. The cavity has very steep walls due to the high spall rates.

Figures 6 and 7, Case C and D, show the influence of spalling on cavity development when ash permeabilities are very low, $10^{-5}k_{ref}$. Case C, without spalling, shows the formation of a cavity which is mainly formed low in the coal region and spread widely. Case D, with a high spall rate, shows a cavity with an irregular shape with steep coal walls, and a large coal zone in the center of the region which is bypassed.

Case E, Fig. 8, with an average spall rate of (21/256) and ash permeability (k_{ref}), shows similar behavior as Case B, only less pronounced. Case F, Fig. 9, shows the developed cavity for a homogeneous permeability field. Here a more or less symmetrical cavity develops without influence of ash permeability or spall rate.

In Case G, Figs. 10 and 11, the influence of a high permeable zone connecting injector and producer is studied. This is an idealized representation of a link obtained by hydraulic fracturing. Fig. 10 shows that a symmetrical cavity develops in the coal, albeit that it is more concentrated around the high permeable linkage zone. Fig. 11 shows two pictures of the 3D velocity field inside the domain. The high permeable linkage zone ($10^{5}k_{ref}$) at $W/2$ is indicated with a narrow band of lines around the coal domain. The left picture shows the initial velocity field, the one on the right shows the velocity field after 40% of the coal has been gasified. The difference in velocity distribution is caused mainly by the fact that a void space with a very high permeability ($10^{5}k_{ref}$) is formed, leading to a more even velocity distribution, and higher velocities higher up in the cavity. Another aspect is that when coal near the linkage zone is gasified a corresponding amount of ash is released, effectively blocking the flow path below it. This also causes the cavity to grow upwards.

Conclusions

1. We have developed a 3D model for underground coal gasification which incorporates natural convection driven coal surface gasification and permeable bed gasification together with temperature and stress induced failure of both rock and coal.

2. Simulation results show that an enhanced spall rate leads to a cavity rapidly growing upwards to the roof rock, with steep coal walls.

3. A low permeable ash layer forming at the bottom of the cavity leads to the bypassing of considerable amounts of coal.

4. A zone of high permeability between injector and producer leads to the initial formation of a single channel at the bottom of the coal zone, but ash clogging will cause sideward and upward expansion of the channel to form a cavity at later stages.

Nomenclature

a = projected area on a horizontal plane
$\mathcal{D}$ = molecular diffusion coefficient, L^2/t, m^2/s
f = oxygen fraction
h = height of coal layer, L, m
j = mass flux, m/L^2t, kg/m^2s
$\vec{j}$ = mass flux vector, m/L^2t, kg/m^2s
k = permeability, L^2, m^2
k_f = mass transfer rate constant, L^3/L^2t, m^3/m^2s
$\mathbf{K}$ = averaged conductivity tensor, t, s
L = length of coal layer, L, m
m = normalization factor
M = molecular weight, m / mole, kg / mole
$\mathcal{N}$ = number of pairs of random numbers
p = pressure, m/Lt^2, Pa
P = mole carbon/mole O_2
Q = total flow rate, L^3/t, m^3/s
$\vec{q}$ = specific discharge, L / t, m / s
r = reaction rate, m/L^2t, kg/m^2s
R = gas constant, $m\,L^2/t^2\,T$, J / mole K
$\mathcal{R}$ = random number
Ra = Rayleigh number
t = time, t, s
t_p = project time, t, days
T = temperature, T, K
W = width of coal layer, L, m
γ = interface height, L, m
Γ = interface
λ = spall factor, L / t, m / s
μ = dynamic viscosity, m / Lt, Pa s
ν = volume ash/volume coal, L^3/L^3, m^3/m^3
ρ = density, m/L^3, kg/m^3
ς = volume ash/volume rock, L^3/L^3, m^3/m^3
χ = mass flux ratio, m / m, kg / kg
ω = volume coal/unit mass gas, L^3/m, m^3/kg
Ω = domain

Subscripts

A = ash region
ac = ash/coal
c = coal
C = coal region
d = downstream
n = normal vector component
r = rock
R = roof-rock region
ref = reference
u = upstream
V = void region
va = void/ash
vc = void/coal
vr = void/rock
x = x-direction (horizontal)
y = y-direction (horizontal)
z = z-direction (vertical)

Acknowledgments

This study has been performed under contract with Novem, The Netherlands' agency for energy and the environment, in the framework of the Underground Coal Gasification Programme, which is financed by The Netherlands' Ministry of Economic Affairs. We thank dr ir D.W. van Batenburg, prof. dr ir J. Hagoort, and dr ir R.J.M. Huijgens for many useful suggestions and critical reading of the manuscript. Finally we thank M.J. King for pointing out the possible extension of the probabilistic method to 3D.

References

[1] Schreurs, H., Biezen, E., Bruining, J., and Wolf, K.-H.: "Economical exploitation of coalbed methane," In *Proceedings of the United Nations international conference on coalbed methane*, Beijing, China. (October 1995).

[2] Hill, R.: "Burn cavity growth during the Hoe Creek no. 3 underground coal gasification experiment," In *Proc. Seventh Annual Underground Coal Gasification Symposium*, (September 1981) p. 19–43. Fallen Leaf, CA.

[3] Thorsness, C. and Britten, J.: "Analysis of material and energy balances for the Rocky Mountain I UCG field test," In *Proc. International Underground Coal Gasification Symposium 1989*, (October 1989) p. 118–134. Delft, The Netherlands.

[4] Dana, G., Covell, J., and Oliver, R.L. Elliott, J.: "Preliminary results of postburn coring and drilling at WIDCO-CRIP UCG experimental test site, Centralia, Washington," In *Proc. Tenth Annual Underground Coal Gasification Symposium*, (August 1984) p. 130–135. Williamsburg, Virginia.

[5] Britten, J. and Thorsness, C.: "A model for cavity growth and resource recovery during underground coal gasification," *In Situ*13(1&2), (1989) p. 1–53.

[6] Chang, H., Himmelblau, D., and Edgar, T.: "Modeling and simulation of self-gasification of coal," *In Situ*9(2), (1985) p. 149–184.

[7] Creighton, J.: "Effects of gas flow pattern on cavity shape," In *Proc. Seventh Annual Underground Coal Conversion Symposium*, (September 1981) p. 199–212. Fallen Leaf, CA.

[8] Eddy, T. and Schwartz, S.: "A side wall burn model for cavity growth in underground coal gasification," *Journal of Energy Resources Technology*105(6), (June 1983) p. 145–155.

[9] Harloff, G.: "A two-dimensional model of UCG-cavity growth with application to the Canadian Forestburg test of 1976," In *Proc. Seventh Annual Underground Coal Conversion Symposium*, (September 1981) p. 213–227. Fallen Leaf, CA.

[10] Van Batenburg, D., Biezen, E., and Bruining, J.: "A new channel model for underground gasification of thin deep coal seams," *In Situ*18(4), (1994) p. 419–451.

[11] Van Batenburg, D.: "Heat and mass transfer during underground gasification of thin deep coal seams," PhD thesis, Dietz Laboratory, Delft University of Technology, (December 1992).

[12] Biezen, E., Bruining, J., and Molenaar, J.: "An integrated model for underground coal gasification," In *Proceedings SPE annual technical conference and exhibition*, New Orleans, LA, USA. (September 1994) p. 191–202. SPE 28583.

[13] Weast, R. and Astle, M., editors. "Handbook of Chemistry and Physics," . CRC, (1978).

[14] Patterson, L.: "Diffusion limited aggregation and two fluid displacements in porous media," *Phys.Rev.Lett.*52(14), (1984) p. 1621–1624.

[15] DeGregoria, A.: "A predictive Monte Carlo simulation of two-fluid flow through porous media at finite mobility ratio," *Phys.Fluids*28(10), (1985) p. 2933–2935.

[16] King, M. and Scher, H.: "Probabilistic stability analysis of multiphase flow in porous media," In *Proc. SPE Annual Conference and Exhibition*, (September 1985).

[17] King, M.: "Viscous fingering and probabilistic simulation," In Wheeler, M., editor, *Numerical simulation in oil recovery*, volume 11 of *IMA*. Springer Verlag, (1988) p. 161–176.

[18] Frick, T. and Zolotukhin, A.: "Field-scale stochastic simulation of IOR processes," In *Proc. 7th European IOR Symposium*, Moscow, Russia. (October 1993).

[19] Kuyper, R.: "Transport Phenomena in Underground Coal Gasification Channels," PhD thesis, Faculty of Applied Physics, Section Heat Transfer, Delft University of Technology, (June 1994).

[20] Tantekin, S., Krantz, W., and Sperry, D.: "Characterization of the overburden spalling properties for the Rocky Mountain I UCG field test site," In *Proc. Thirteenth Annual Underground Coal Gasification Symposium*, (August 1987) p. 408–416. Laramie, Wyoming.

[21] Godderij, R. and Bruining, J.: "A new model to predict steam override and viscous fingering in heterogeneous oil reservoirs," In *Proceedings Western Regional meeting*, Bakersfield, CA, USA. (March 1995) p. 459–471. SPE 29661.

[22] Van Batenburg, D. and Bruining, J.: "The efficiency of filtration gasification," *In Situ*17(4), (1993) p. 413–437.

[23] Christie, M. and Bond, D.: "Detailed simulation of unstable processes in miscible flooding," *SPE Res.Eng.*2(4), (1987) p. 514–522.

[24] Press, W., Flannery, B., Teukolsky, S., and Vetterling, W.: "Numerical recipes in C," . Cambridge University Press, (1988).

[25] Molenaar, J.: "A simple and efficient multigrid method for interface problems," In Peters, A., editor, *Computational methods in water resources X*. Kluwer Academic Publishers, (1994) p. 1425–1431.

[26] Molenaar, J.: "A simple multigrid method for 3D interface problems," Technical Report 94-44, TU Delft-TWI, (1994).

Appendix–Solution of the equation of motion by the probabilistic method

The procedure described here is an extension of the procedure given by King.[17] The domain is subdivided in $N_x \times N_y \times N_z$ grid blocks of size $\Delta x \times \Delta y \times \Delta z$. In the calculations shown we use cubical grid blocks ($\Delta x = \Delta y = \Delta z$). Each grid block may contain a few horizontal layers of e.g. coal, rock, charred coal, void, or ash/spalled rock. The different components (coal etc.) are indicated in Fig. 1. Most grid blocks contain a single component. Grid blocks in the vicinity of the interfaces Γ_{ac} and Γ_{vc}, however, may consist of two and in some cases three components. Void cannot be overlain by ash and spalled rock.

The approximate interface heights $\tilde{\gamma}_{\alpha\beta}(x,y,t_l)$ are piecewise constant on the square with corners $(n\,\Delta x, m\,\Delta y)$ and $((n+1)\Delta x,(m+1)\Delta y)$, m=0,1,..., n=0,1,..., and calculated for times t_l, l=0,1,.... In each time step $\Delta t_l = t_{l+1} - t_l$ the following events occur. First, a coal block of volume Δx^3 is gasified. Secondly, a certain amount of coal is gasified by cavity gasification. Thirdly, a coal block may spall and is subsequently gasified. Finally, a piece of rock may spall. The time Δt_l is calculated from the air injection rate and the amount of coal gasified. As a result of these events the interface height $\tilde{\gamma}_{\alpha\beta}(x,y,t_{l+1})$ is determined from the interface height $\tilde{\gamma}_{\alpha\beta}(x,y,t_l)$ as follows. First we calculate the total flow, Q, *through all coal/char faces which are exposed to either void or ash*. Then we use a random number generator[24] to draw a single random number, $\mathcal{R}_1$, uniformly distributed between zero and one. Subsequently, we repeat the summation *through the exposed coal and char faces* until the value $\mathcal{R}_1 Q$ is reached. The coal block nearest to the intersection point with height Δx is removed. Either the interface $\tilde{\gamma}_{ac}$ is lowered by Δx or the interface $\tilde{\gamma}_{vc}$ is moved up by Δx at this position. The coal near the interfaces $\tilde{\gamma}_{ac}$ and $\tilde{\gamma}_{vc}$ that have the highest mass flux has the highest probability to be gasified. This method is based on the fact that the velocity values plotted along the interface can be interpreted as a cumulative distribution function.[17,24] The interface $\tilde{\gamma}_{vc}$ is further moved due to natural convection driven cavity gasification in a deterministic fashion: all horizontal faces of $\tilde{\gamma}_{vc}$ are moved upward by an amount proportional to the added coal surfaces of the block under consideration and all exposed blocks vertically above it. The constant of proportionality is the natural convection driven transfer rate $r/\rho_{coal}\Delta t_l$.

A second and third random number $\mathcal{R}_2$ and $\mathcal{R}_3$ are drawn and multiplied by L and W, respectively, at specific intervals within each time step, depending on the coal spall rate. $(\mathcal{R}_2 L, \mathcal{R}_3 W)$ is an x,y-location that specifies a column of grid blocks. If this column intersects with Γ_{vc} it indicates a position where coal spalling takes place. The interface $\tilde{\gamma}_{vc}$ at the position of the column is moved upwards by Δx. A fourth and fifth random number $\mathcal{R}_4$ and $\mathcal{R}_5$ are drawn at specific intervals, depending on the rock spall rate. $(\mathcal{R}_4 L, \mathcal{R}_5 W)$ is an x,y-location that specifies a column of N_z grid blocks. If this column intersects with Γ_{vr}, it indicates a position where rock spalling takes place. The interface $\tilde{\gamma}_{vr}$ at the position of the column is moved upward by Δx. Finally, $\tilde{\gamma}_{va}$ is moved as a weighted sum of the movement of all other interfaces according to Eq. 5.

Calculation of the flow field. Grid blocks have average permeability values. Therefore, we need an averaging procedure in each grid block for the conductivity $\frac{\rho k m}{\mu}$. The averaged conductivity **K** becomes a tensor. The horizontal (both the x and the y-direction) and vertical (the z-direction) conductivity values are arithmetic and harmonic averages respectively. Therefore the upscaled pressure Eq. 4 becomes

$$\text{div}\ \mathbf{K}\cdot\mathbf{grad}\,p = 0\,, \qquad \text{in } \Omega \ldots\ldots\ldots\ldots\ldots\ldots (A-1)$$

K has zero off-diagonal terms owing to the assumption that the permeability components form a horizontally layered structure.

TABLE 1–INPUT PARAMETERS COMMON TO ALL SIMULATIONS

Constant	Value	Unit
$\mathcal{D}$	$1 \cdot 10^{-5}$	m^2/s
f	0.21	–
h	4	m
k_f	$2.8 \cdot 10^{-3}$	m^3/m^2s
L	8	m
M_c	0.012	kg / mole
p	$5 \cdot 10^6$	Pa
P	2	mole / mole
r	$1.41 \cdot 10^{-4}$	kg/m^2s
t_p	10	days
T_d	1673	K
T_u	313	K
W	8	m
μ_u / μ_d	0.35	–
ν	0.5	m^3/m^3
ρ	1300	kg/m^3
ς	1.0	m^3/m^3
χ	1.14	kg/kg
ω	$1.33 \cdot 10^{-4}$	m^3/kg

TABLE 2–VARIATION IN INPUT PARAMETERS FOR EXAMPLE CALCULATIONS

Case	Spall rate [-]	k_{ash} $[k_{ref}]$	k_{coal} $[k_{ref}]$	k_{rock} $[k_{ref}]$	k_{void} $[k_{ref}]$
A	0	10^5	1	10^{-3}	10^5
B	50/256	10^5	1	10^{-3}	10^5
C	0	10^{-3}	1	10^{-3}	10^5
D	50/256	10^{-3}	1	10^{-3}	10^5
E	21/256	1	1	10^{-3}	10^5
F	0	1	1	1	1
G[1]	0	1	10^{-3}	10^{-3}	10^5

[1] a high permeable ($10^5 k_{ref}$) zone links injector and producer

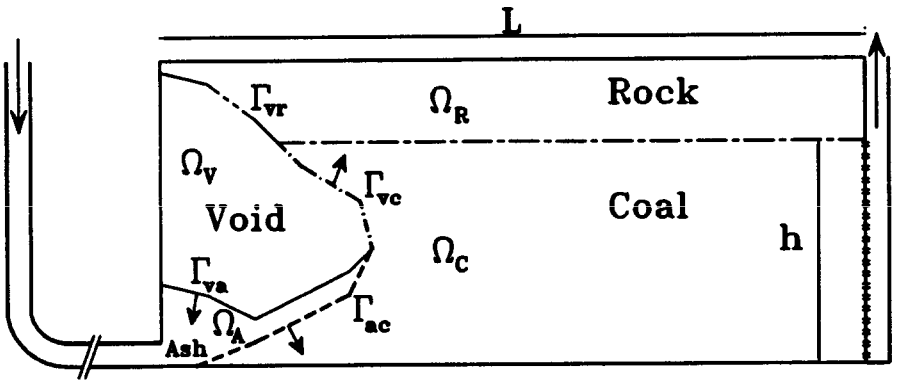

Fig. 1–Vertical cross-section at $W/2$ with the different regions of interest.

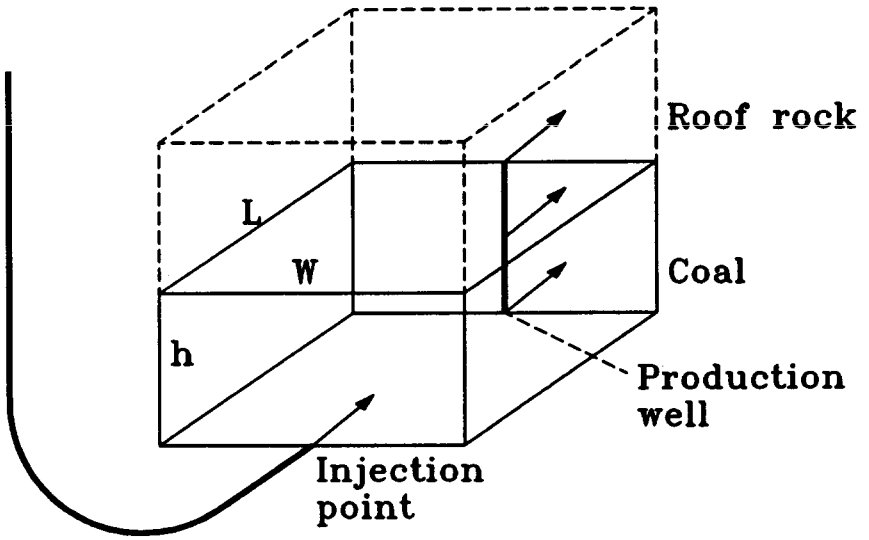

Fig. 2–A 3D schematic of a coal layer with overlying roof rock, including well-layout during the first CRIP step. It should be noted that injection occurs from the tip of a horizontally drilled well.

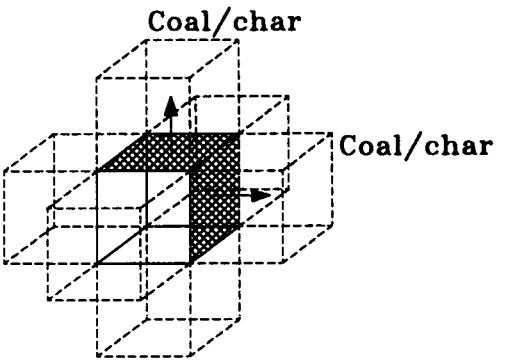

Fig. 3–From a single void or ash location (center cube) all flows through each of the cubes' faces are added, if the adjacent block is char or coal.

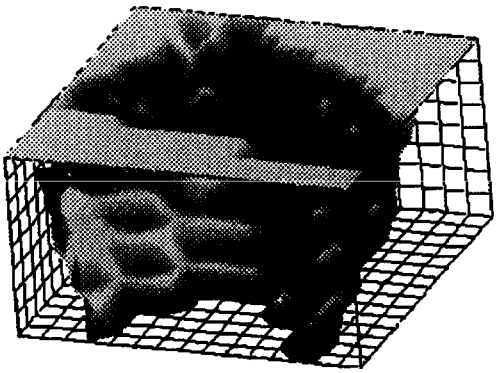

Fig. 4–Case A: 3D view showing the gasified region, after 40% of the coal has been gasified. The spall rate is 0, ash permeability is $10^5 k_{ref}$, and ash content is 50%. The injection/production well layout is shown in Fig. 2.

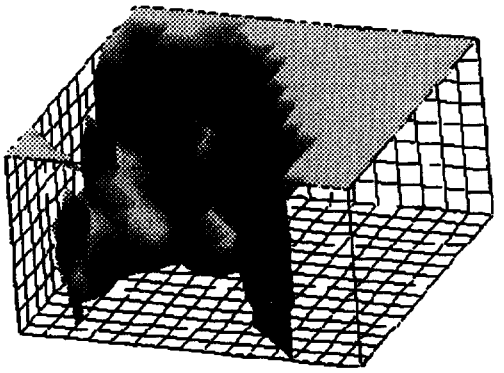

Fig. 5–Case B: 3D view showing the gasified region, after 40% of the coal has been gasified. The spall rate is 50/256, ash permeability is $10^5 k_{ref}$, and ash content is 50% The injection/production well layout is shown in Fig. 2.

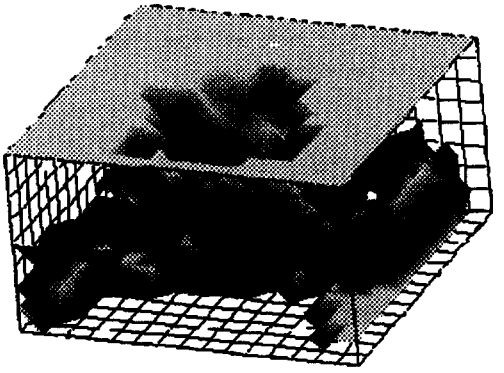

Fig. 6–Case C: 3D view showing the gasified region, after 40% of the coal has been gasified. The spall rate is 0, ash permeability is $10^{-3} k_{ref}$, and ash content is 50% The injection/production well layout is shown in Fig. 2.

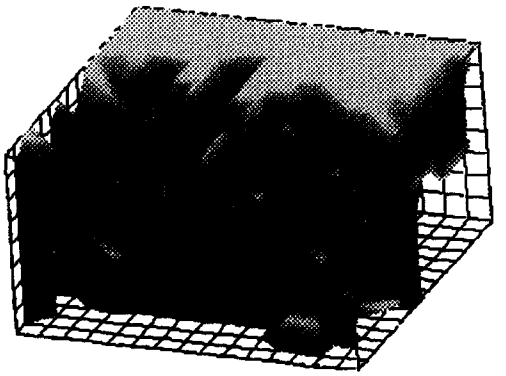

Fig. 7–Case D: 3D view showing the gasified region, after 40% of the coal has been gasified. The spall rate is 50/256, ash permeability is $10^{-3}k_{ref}$, and ash content is 50% The injection/production well layout is shown in Fig. 2.

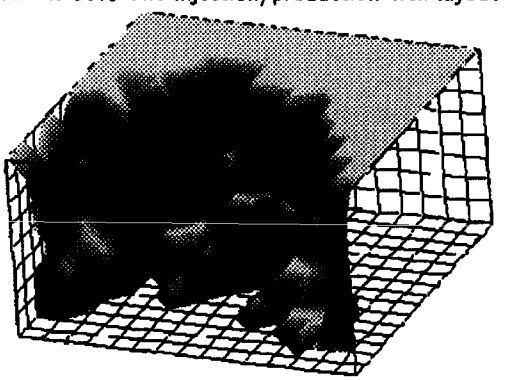

Fig. 8–Case E: 3D view showing the gasified region, after 40% of the coal has been gasified. The spall rate is 21/256, ash permeability is k_{ref}, and ash content is 50% The injection/production well layout is shown in Fig. 2.

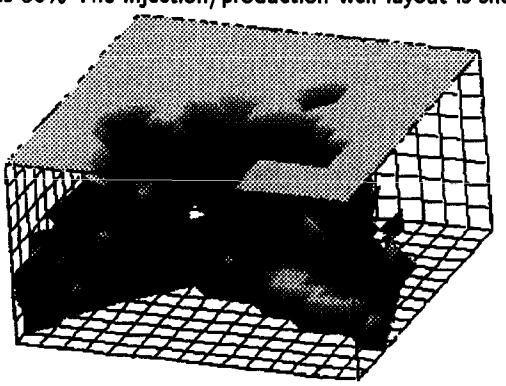

Fig. 9–Case F: 3D view showing the gasified region, after 40% of the coal has been gasified. The spall rate is 0, ash permeability is k_{ref}, and ash content is 50% The injection/production well layout is shown in Fig. 2.

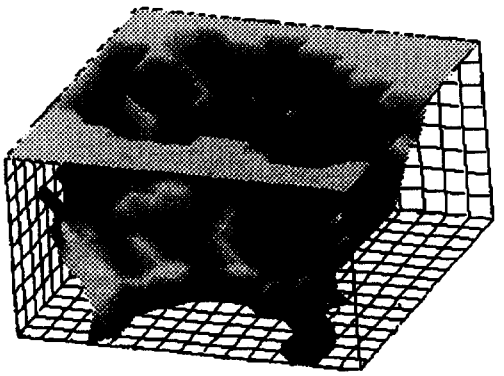

Fig. 10–Case G: 3D view showing the gasified region, after 40% of the coal has been gasified. The spall rate is 0, ash permeability is k_{ref}, and ash content is 50%. The injection/production well layout is shown in Fig. 2 At W/2 a high permeable region links injector and producer.

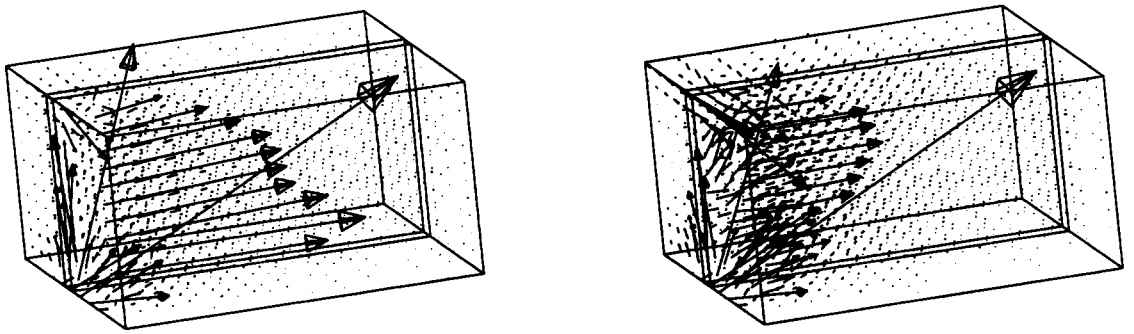

Fig. 11–Case G: Two 3D views from the side (injection at the left of the domain, production at the right) showing the initial velocity distribution in the left picture, and the velocity distribution after 40% of the coal has been gasified in the right picture. The vertical high permeable linkage zone at $W/2$ is indicated with a band around the coal domain. The two large arrows in each of the pictures indicate the high velocities near the injection point.